Determination of diffusion lengths in organic semiconductors: Correlation with solar cell performances

Christophe Longeaud, Amir Fath Allah, Javier Schmidt, Mustapha El Yaakoubi, Solenn Berson, Noëlla Lemaitre

Determination of diffusion lengths in organic semiconductors: correlation with solar cell performances

Christophe Longeaud[1,*], Amir Fath Allah[1], Javier Schmidt[2], Mustapha El Yaakoubi[3], Solenn Berson[4], Noëlla Lemaitre[4]

[1] GEEPS – CNRS, CentraleSupelec, UPSud, UPMC, 11 rue Joliot Curie, 91192 Gif sur Yvette, France
[2] IFIS-Litoral, Güemes 3450, S3000GLN Santa Fe, Argentine
[3] TFSC-Instrument, 3 Rue Léon Blum, 91120 Palaiseau, France
[4]Université Grenoble-Alpes, INES, F-73375, Le Bourget du lac, France
CEA, LITEN, Department of Solar Technologies, F-73375 Le Bourget du lac, France
* Corresponding author : longeaud@geeps.centralesupelec.fr

Organic semiconductors are promising candidates for future applications in solar energy conversion. Recent investigations of bulk heterojunction (BHJ) semiconductors have suggested a density of states and transport mechanisms by multiple trapping close to those observed in disordered inorganic thin films. That is why we have applied to BHJ thin films experiments that are currently used for disordered semiconductors. In addition to the steady state photoconductivity we have tested the ability of the steady state photocarrier grating (SSPG) technique to provide information on the minority carrier diffusion length. We found that SSPG can be applied to P3HT:PCBM thin films leading, for the best sample, to a diffusion length of the order of 125 nm. From the comparison of the transport parameters obtained on thin films with the performances of the devices integrating the latter, we conclude that SSPG is a very powerful tool for optimizing the BHJ thin film properties before their incorporation in solar devices.

Keywords: Organic semiconductors, transport properties, solar cells

1. Introduction

Organic bulk heterojunction (BHJ) semiconductors have received a growing attention in the last decade for they may constitute the basic absorbers of tomorrow solar cells. These absorber layers are made of a blend of phase-separated electron acceptors and donors and the transport of carriers occurs in these different domains with interaction of these carriers with the density of states (DOS). Determination of the DOS distribution and identification of the transport mechanisms still remain a matter of debate and several models have been proposed [1, 2]. Most of these models rely on the study of the drift mobility measured by time-of-flight experiments and its behaviors with respect to applied field and temperature. Photoconductivity studies by R. A. Street *et al*. have widen the field of investigations by the measurement of spectral photoresponse [3] on solar cells based on P3HT:PCBM and PCDTBT:PC_{70}BM absorbers [4]. In addition, transient photoconductivity and photovoltage techniques have been applied to the same materials and devices [5]. On the basis of their experimental results

these authors have proposed a model for the DOS in BHJ. The DOS is based on the properties of both materials incorporated in the cell: the highest occupied molecular orbital (HOMO) being assimilated to the valence band of inorganic semiconductors and the lowest unoccupied molecular orbital (LUMO) being assimilated to the conduction band of inorganic semiconductors. Transient photoconductivity has revealed an exponential band tail followed by a flatter distribution of deep states. As underlined by R. A. Street, transient photoconductivity has been used to study low mobility transport inorganic materials as hydrogenated amorphous silicon (a-Si:H) [6]. Some procedure based on Laplace transform was even proposed to extract the DOS distribution from post-transit time of flight currents [7]. It is beyond doubt that a similarity exists between the behaviors observed in both types of materials (BHJ and a-Si:H) in which multiple trapping in localized states seems to control transport phenomena [3]. The review of transport phenomena in polymers by S. Baranovski is also in favor of this similarity [8]. That is why we wondered if other experiments could be applied to BHJ materials to gain more insight in the material properties and therefore could be a help in the optimization of solar devices. A rather large number of experiments have been dedicated to the study of transport parameters in semi-insulating and semiconducting thin film materials, most of them based on their photoconductivity property. Only the light excitation spatial and temporal 'shape' is varied from one experiment to the other. The aim of this communication is not to achieve a detailed review of all the techniques and the reader may have a look at the references 9 to 13. The simplest technique is the steady-state photoconductivity (SSPC) in which one measures the evolution of the film photoconductivity with temperature and/or a steady generation rate. From this experiment one can deduce the dark conductivity of the material and a mobility-lifetime product under illumination. The illumination of the film can also be spatially modulated by means of a light grating created by two interfering laser beams. The simplest experiment uses a steady grating as in the steady state photocarrier grating (SSPG) [10], from which one deduces the ambipolar diffusion length of the carriers.

In this communication we shall concentrate on the SSPC and SSPG techniques applied to P3HT:PCBM thin films and compare the parameters deduced from these experiments to the performances of solar devices containing the same layers as absorbers.

2. Experimental details

First, it has to be underlined that SSPC and SSPG techniques are applied to samples built in coplanar geometry. Films are deposited on top of an insulating substrate and two parallel electrodes are subsequently deposited on the thin film with a spacing of 1 mm. Problems of transport anisotropy can then be encountered for instance in the case of micro-crystalline silicon. Due to columnar growth of the crystallites, the transport parameters can be very different when measured alongside or perpendicularly to the substrate [14-16]. In the case of organic films, we could also expect transport

anisotropy even alongside the substrate if the films were prepared with an alignment of the molecules in a preferential direction [17, 18]. However, in the case of BHJ thin films prepared by spin coating, as it is the case here, the disorder of the intermixed phases should prevent the occurrence of transport anisotropy and we are quite confident that the transport parameters we deduced from our experiments, with current flowing parallel to the substrate, are the same that could be measured with current flowing perpendicularly to the substrate as in solar devices.

2.1. Samples preparation

The films for SSPG and bulk heterojunction active layers, 200 nm thick, were fabricated from a P3HT:$PC_{60}BM$ solution in anhydrous 1,2-dichlorobenzene (99%, from Sigma-Aldrich) (concentration in P3HT : 26 g/l) by spin coating. P3HT and $PC_{60}BM$ were purchased from Merck. One series was achieved with different ratios of P3HT and PCBM : 1:0.3, 1:0.6, and 1:1 respectively. These films were annealed 10 min at 140 °C under nitrogen atmosphere. In addition, a series of films with a ratio of 1:0.6 was deposited without annealing or with an annealing at 100 °C during 10 min under nitrogen atmosphere. For the coplanar samples, films were deposited on glass substrates, pre-cleaned by a UV-ozone treatment, and then covered with different types of metal to achieve parallel electrodes separated by 1 mm spacing: i) 150 nm of aluminum, ii) 10 nm of gold covered with 150 nm of silver and iii) 160 nm of silver alone. The ohmicity of the contacts was checked prior to the measurements with applied voltage up to 32 volts. The measurements were performed with a voltage fixed at 20 V. The films were deposited at INES and studied at GEEPS. They were sent from INES in sealed nitrogen atmosphere to avoid any oxygen or water vapor contamination. At reception and during all the measurements at GEEPS, the films were kept under vacuum in a dynamically pumped cryostat (< 10^{-3} Pa) in order to avoid any contamination.

Organic solar cells were fabricated on pre-etched glass/ITO substrates with the structure: Glass / ITO / PEDOT: PSS / P3HT : PCBM active layer / Ca /Al. The substrate was pre-cleaned by a UV-ozone treatment for 30 min in air. Hole Transporting Layer (HTL) was spin-coated using PEDOT:PSS (Baytron-PH) annealed for 30 min at 180°C in air. The active layer was prepared as for the SSPC and SSPG samples. Finally, a cathode of calcium and aluminum, 200 nm thick, was evaporated at 10^{-3} Pa through a shadow mask. This leads to solar cells with an active surface of 28 mm^2. The fill factor, short circuit current, open circuit voltage and power conversion efficiency were deduced from I(V) measurements. These measurements were carried out under nitrogen atmosphere using AM 1.5, 100 mW/cm^2 illumination, obtained by an Oriel SP94043A (Xe Lamp) Solar simulator. Characteristics and power conversion efficiencies were measured via a computer controlled Keithley SMU 2400 unit. A monocrystalline silicon solar cell, calibrated at the Fraunhofer Institut für Solare Energie Systeme (Freiburg, Germany), was used as a reference cell to confirm stabilization of the 100 mW/cm^2 illumination. The used apparatus was a standard system that is widely used and gives a relative error

(mismatch factor) of around 5% on the estimated power conversion efficiency in the 300 to 1100 nm range in comparison with AM1.5G. The mismatch factors were measured using a spectrophotometer AECUSOFT, from Flashspec.

2.2 Characterisations

We have recently built a bench on which SSPC and SSPG measurements can be performed automatically [19] the sample being maintained under vacuum. The light illuminating the film is emitted by a He-Ne laser (633 nm). For both techniques, SSPC and SSPG, we have used a rather high flux of 3×10^{16} cm^2s^{-1}. All the measurements presented here were done at room temperature.

With the SSPC technique we have investigated the ohmicity of the contacts and, when it was the case, we have deduced from these measurements the dark conductivity σ as well as the mobility-lifetime product $\mu\tau$ of the majority carriers. As far as organic polymers are concerned the notions of majority and minority carriers may be somewhat different from those used in inorganic semiconductors, particularly the doped ones. However, even in undoped inorganic semiconductors there is often one type of carrier that gives a major contribution to the current, dark or photocurrent, because either the carriers of this type are more numerous or more mobile or both. The same behavior is probably encountered in BHJ materials and in the following we shall call 'majority' carriers those which mostly contribute to the steady photocurrent, the 'minority' ones being the less mobile for instance.

The SSPG technique was first proposed by D. Ritter and coworkers [10]. It is one of the few experiments from which one can study the influence of the minority carriers on the transport of the majority ones and eventually deduce the diffusion length L_d of minority carriers. The SSPG basic idea is to split a laser beam of wavelength λ into two beams subsequently deflected to illuminate the sample in between the contact electrodes, the polarization of each beam being parallel to the electrodes, and each beam presenting an angle $\theta/2$ with the perpendicular to sample plane. Under these conditions an array of interferences is created in the sample with a grating period Λ given by the equation

$$\Lambda = \frac{\lambda}{2\sin(\theta/2)} \quad . \tag{1}$$

One of the beams, the probe beam, is attenuated by a factor of the order of 30, compared to the other one, the main beam, that fixes the equilibrium steady state of the sample. As a consequence of the interferences two arrays of space charge develop in the sample: an array linked to the majority carriers and another one linked to the minority carriers. These two arrays should disappear by diffusion and, each of them acting onto the other because of the opposite charge, the diffusion to be taken into account is the ambipolar one controlled mostly by the slowest carrier. If these arrays are not swept and

blurred by drift and diffusion, they may influence and alter the majority carrier transport under the applied external field. It must be underlined that the very same limitation of transport occurs in a solar device if the minority carriers are not extracted while created. Hence, the SSPG technique is particularly interesting for measuring diffusion lengths L_d of thin films to be integrated in solar cells. If the SSPG technique is performed at high flux, the L_d measured will be close to that of the material in an operating solar cell. Therefore, materials presenting a high diffusion length measured with SSPG are worth to be used as an absorber whereas materials presenting a low diffusion length compared to their thickness will always lead to solar cells with poor efficiency. That is why this technique was used to study a large variety of materials (for a review see [20]).

To determine L_d the probe beam is chopped at a low frequency, say a few tens of Hz or so, and one measures the current resulting from the influence of this beam with a lock-in amplifier. The current with interferences I_{wi} and the current without interferences I_{woi} are measured for different values of Λ and a plot of the quantity

$$\beta(\Lambda) = \frac{I_{wi}}{I_{woi}} = 1 - \frac{2\phi}{\left[1 + (2\pi L_d / \Lambda)^2\right]^2} \quad , \qquad (2)$$

gives an estimate of L_d by fitting the curve $\beta(\Lambda)$. The parameter ϕ, usually lying between 0.5 and 1, depends on the contrast of the interferences, the intensity dependence of the photocurrent on the light flux and the ratio between dark current and total current under illumination [10]. The grating period Λ is modified by changing the angle between the two beams, and the interferences are suppressed by rotating the polarization of one beam to set it perpendicular to that of the second beam. Eq. (2) assumes that the diffusion is purely ambipolar and under some circumstances it may not be the case. That is why some authors, Balberg *et al.* [21], have recommended using the following equation

$$1/\Lambda^2 = \left(\frac{1}{2\pi L_d}\right)^2 \left(\phi^{1/2}\left(2/(1-\beta)\right)^{1/2} - 1\right), \qquad (3)$$

which is another way to write Eq. (2) and should give a linear plot of the variations of $1/\Lambda^2$ as function of $\left(2/(1-\beta)\right)^{1/2}$. This linear plot presents the advantage to underline any disagreement with the theory since any deviation from linearity can be easily identified. For instance, ambipolarity condition is not satisfied if the external applied field is too high [22] leading to a bending of the straight line.

3. Results and discussion

When studying the contacts ohmicity, we have found that aluminum had to be rejected for the purpose of contact electrode. We did not observe any ohmicity neither under dark nor under light

conditions. Aluminum appears to be a blocking contact for one type of carriers and we have always observed a very slow increase of the current flowing into the film when shifting from one bias to another, this current never reaching the expected value if the contact was ohmic, even after waiting more than an hour. On the other hand we did observe an ohmic behavior either with the stack of gold and silver contacts or with silver layers alone with no significant differences in the parameters we measured, that could be linked to the nature of the contacts. Table I summarizes our results. One can see that the dark conductivities σ are in a large range between $6.6\text{x}10^{-7}$ and $1.6\text{x}10^{-5}$ S/cm and depend on the annealing temperature, the higher the temperature the higher σ, and on the proportion of PCBM in the blend, the higher the quantity of PCBM the lower σ.

P3HT :PCBM	1:0.6	1:0.6	1:0.6	1:0.3	1:1
T Anneal (°C)	No	100	140	140	140
σ (S/cm)	$6.6\text{x}10^{-7}$	$1.5\text{x}10^{-6}$	$9.8\text{x}10^{-6}$	$1.6\text{x}10^{-5}$	$1.5\text{x}10^{-6}$
μτ (cm^2/V)	$0.54\text{x}10^{-7}$	$0.94\text{x}10^{-7}$	$1.90\text{x}10^{-7}$	$7.4\text{x}10^{-7}$	$0.7\text{x}10^{-7}$
L_d (nm)	75	115	125	50	110
$\mu\tau_{amb}$ (cm^2/V)	$1.12\text{x}10^{-9}$	$2.64\text{x}10^{-9}$	$3.12\text{x}10^{-9}$	$0.50\text{x}10^{-9}$	$2.42\text{x}10^{-9}$

Table I Summary of the different parameters measured on P3HT:PCBM blends prepared under different conditions.

As mentioned above we have developed a bench on which SSPG can be performed automatically [19]. With this bench we can vary the grating period from 1 µm to 24 µm in 9 different steps, a range large enough for the studied samples. A cryostat has been adapted to this bench so that experiments can be conducted under vacuum to avoid any contamination of the films. The diffusion lengths deduced from our measurements are listed in Table I. The ambipolar mobility-lifetime products $\mu\tau_{amb}$ associated to these L_d can be extracted from the equation [20]

$$L_d = \sqrt{2\frac{k_b T}{q}\mu\tau_{amb}}\,, \tag{4}$$

and are at least 10 times smaller than the $\mu\tau$ products, also displayed in Table I, that we deduced from the SSPC experiment for all the samples. It shows that $\mu\tau_{amb}$ is almost equal to the mobility-lifetime product of the minority carriers while $\mu\tau$ measured by SSPC can be considered as the mobility-lifetime product of the majority carriers. We have also checked that we obtained a straight line from the 'Balberg' plots. That is why we can assume that L_d is the diffusion length of the minority carriers in the studied films.

The data of Table I ($\mu\tau$ and L_d) are plotted in Fig. 1 as function of the ratio P3HT:PCBM in Fig. 1(a) and as function of the annealing temperature in Fig. 1(b). Below these figures are plotted, in Figs.

1(c) and (d) respectively, the evolutions with the same parameters of the conversion efficiency η and of the fill factor FF of the solar cells made with the same absorbers studied with SSPC and SSPG.

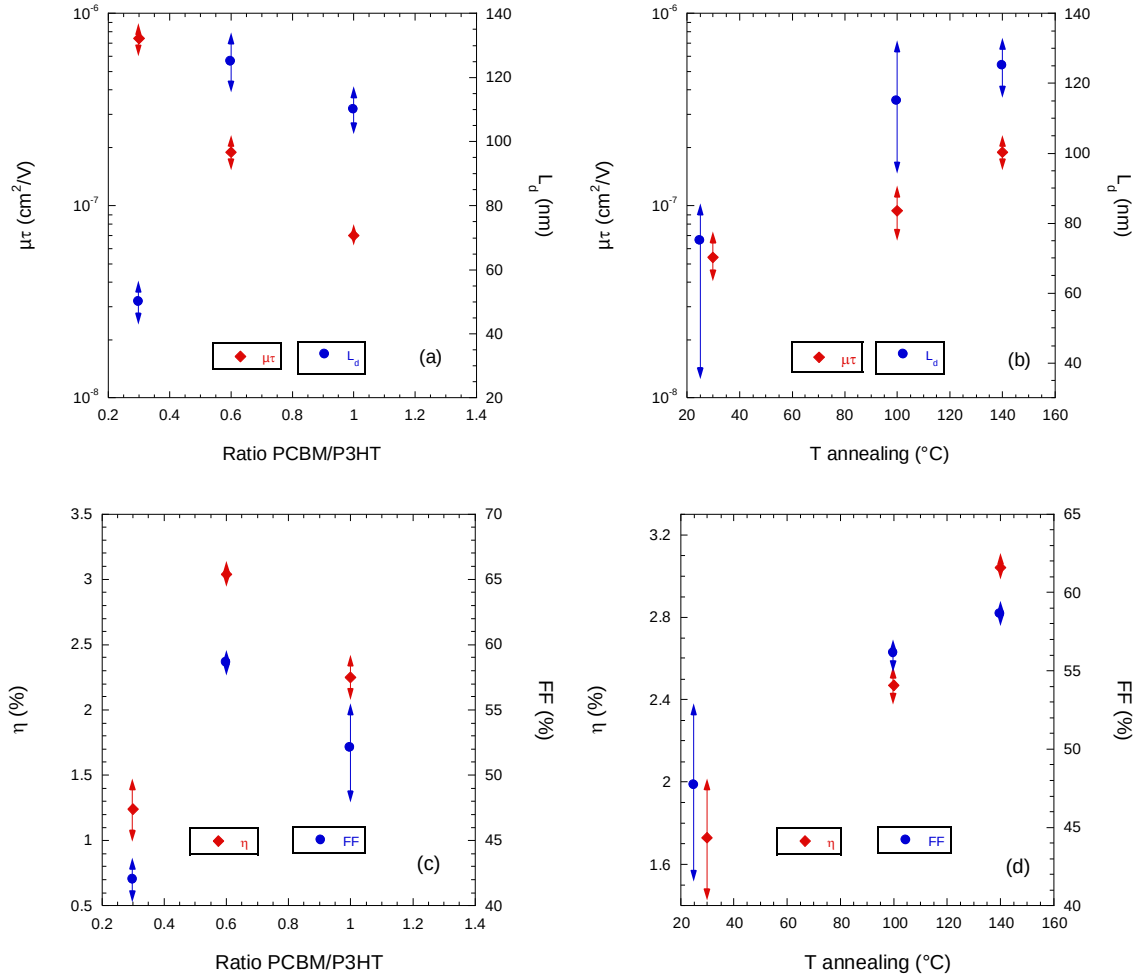

Fig. 1. Evolution of the $\mu\tau$ product measured with SSPC and of the diffusion length L_d (a) with the ratio P3HT:PCBM and (b) with the annealing temperature with a constant ratio of 1:0.6, to be compared with the evolution of the conversion efficiency η and fill factor FF of the corresponding devices shown in (c) and (d). For clarification purpose the abscissa values of the data obtained for samples without annealing have been set at 25 and 30 °C.

One can see that there is an excellent agreement between the parameters of the films deduced from SSPC and SSPG and the quality of the corresponding devices. For instance, the increase of both $\mu\tau$ and L_d with the annealing temperature of the 1:0.6 blend are correlated with an increase of the fill factor and of the conversion efficiency (See Figs. 1 (b) and (d)). The interpretation of the link between Figs. 1 (a) and (c) is a little bit more intricate. If one considers the blends 1:0.3, 1:0.6, and 1:1 it can be seen that the $\mu\tau$ decreases with increasing proportion of PCBM while L_d present a maximum for the 1:0.6 blend. Though $\mu\tau$ is high for the 1:0.3 blend, L_d is small and it leads to a small conversion efficiency and a low fill factor. The 1:1 blend has a lower $\mu\tau$ and a lower L_d than the 1:0.6 blend that explains also a lower fill factor and a lower conversion efficiency than the 1:0.6 blend. This latter

presents then the best compromise between $\mu\tau$ and L_d that gives the best conversion efficiency and fill factor of the series.

Before concluding we would like to add some comments on the results obtained on these films and devices. First, it can be seen in Fig. 1 that the data dispersion is the largest for the samples, films and devices, that were not annealed and that this dispersion decreases with annealing temperature. This shows that annealing is mandatory to obtain both 'good' and reproducible samples. Second, we have not shown the evolution of the measured short circuit current densities J_{sc} with the preparation conditions but they follow the same trends as FF and η. For the samples annealed at 140 °C, the maximum of J_{sc} is reached for the 1:0.6 blend (9.3±0.2 mA/cm^2) and the minimum is obtained for the 1:0.3 blend (5.4±1.7 mA/cm^2), the 1:1 blend giving a value in between (7.9±0.4 mA/cm^2). For the non-annealed 1:0.6 blend J_{sc} is the lowest of the series (6.5±0.4 mA/cm^2) and the 1:0.6 blend annealed at 100 °C gives J_{sc} = 7.9±0.3 mA/cm^2. Considering two devices with the same $\mu\tau$ but with two different $\mu\tau_{amb}$, one would expect to obtain the best J_{sc} with the absorber presenting the largest $\mu\tau_{amb}$: the larger the diffusion length, the better the collection of the minority carriers. With high L_d minority carriers are not piling into the device and do not create a space charge limiting the majority carrier collection. However, devices for which the absorber presents a small $\mu\tau$ cannot present a very high J_{sc} for an obvious reason that is a limited creation of photogenerated carriers. As for FF and η, the best J_{sc} is thus obtained with the film presenting the best compromise between $\mu\tau$ and $\mu\tau_{amb}$. Finally, concerning the open circuit voltage V_{oc} we also observe an optimum for the 1:0.6 blend annealed at 140 °C. However, the various V_{oc} are in a small range (545 ≤ V_{oc} ≤ 560 mV), showing that V_{oc} is less sensitive to L_d than the other device parameters at least in the explored range of preparation parameters. Nevertheless, we would observe a small V_{oc} in the case where the ambipolar diffusion length was also very small. In this case, excessive recombination would limit the quasi Fermi levels splitting that results into a poor V_{oc} as observed in inorganic thin films.

It should be noted that the observed evolution of solar cell parameters with the ratio P3HT:PCBM is in accordance with the results reported recently in the literature by other authors [23]. This confirms that the optimization of the absorbers layers can be performed easily and rapidly with SSPC and SSPG methods prior to solar cell manufacturing.

4. Conclusion

In conclusion we have applied to P3HT:PCBM blends characterization techniques (SSPC and SSPG) that were successfully used for the measurements of transport parameters in several inorganic semiconductors. Though the transport mechanisms are not strictly the same in organic and inorganic semiconductors, these techniques seem to be perfectly applicable to organic blends. The evolution of the transport parameters we have obtained on different types of P3HT:PCBM thin films are in very

good agreement with the performances of the devices, conversion efficiency and fill factor, integrating these films as absorbers. In the future we believe that SSPG could be one of the key tools to be used for optimization of BHJ thin films transport parameters and devices conversion efficiency.

Acknowledgements: This work was partly supported by an ECOS-Sud Project (A13E02).

References

[1] H. Bässler, Phys. Stat. Sol. (b) 175, (1993) 15.

[2] S. V. Novikov, J. Polymer Sci. B 41, (2003) 2584.

[3] R. A. Street, K. W. Song, J. E. Northrup, S. Cowan, Phys. Rev. B 83, (2011) 165207.

[4] PCDTBT is poly[N-9'-hepta-decanyl-2,7-carbazole-alt-5,5-(4',7'-di-2-thienyl-2',1',3'-benzothia-diazole], $PC_{70}BM$ is [6,6]-phenyl C70 butyric acid methyl ester, and P3HT is poly[3-hexylthiophene].

[5] R. A. Street, Phys Rev. B 84, (2011) 075208.

[6] F. W. Schmidlin, Phys. Rev. B 16, (1977) 2362.

[7] G. F. Seynhaeve, R. P. Barclay, G. J. Adriaenssens, J. M. Marshall, Phys. Rev. B 39, (1989) 10196.

[8] S. D. Baranovski, Phys. Stat. Sol. B 251, (2014) pp 487-525.

[9] H. Oheda, J. Appl. Phys. 52, (1981) 6693.

[10] D. Ritter, E. Zeldov, K. Weiser, Appl. Phys. Lett. 49, (1986) 791.

[11] U. Haken, M. Hundhausen, L. Ley, Appl. Phys. Lett. 63, (1993) 3063.

[12] K. Hattori, Y. Koji, S. Fukuda, W. Ma, H. Okamoto, Y. Hamakawa, J. Appl. Phys. 73, (1993) 3846.

[13] C. Longeaud, F. Ventosinos, J. A. Schmidt, J. Appl. Phys. 112, (2012) 023709.

[14] K. Kanahata, T. Lamiya, C. M. Fortmann, I. Shimizu, H. Stuchlikova, A. Fejfar, J. Kocka, J. Non-Cryst. Solids 266-269, (2000) 341.

[15] V. Svrcek, I. Pelant, J. Kocka, P. Fojtik, B. Rezek, H. Stuchlikova, A. Fejfar, J. Stuchlik, A. Poruba, J. Appl. Phys. 89, (2001) 1800.

[16] T. Unold, R. Brüggemann, J. P. Kleider, C. Longeaud, J. Non-Cryst. Solids 266-269, (2000) 325

[17] B. T. O'Connor, O. G. Reid, X. Zhang, R. J. Kline, L. J. Richter, D. J. Gundlach, D. M. DeLongchamp, M. F. Toney, N. Kopidakis, G. Rumbles, Adv. Funct. Mat. 24, (2014) 3422.

[18] L. H. Jimison, M. F. Toney, I. McCulloch, M. Heeney, A. Saleo, Adv. Mat. 21, (2009) 1568.

[19] C. Longeaud, Rev. Sci. Instrum. 84, (2013) 055101.

[20] R. Brüggemann, in chapter 8 of "*Advanced Characterization Techniques for Thin Film Solar Cells*", Edited by D. Abou-Ras, T. Kirchartz and U. Rau, Wiley-VCH Verlag GmbH & Co (2011)

[21] I. Balberg, A. E. Delahoy, H. A. Weakliem, Appl. Phys. Lett. 53, (1988) 992.

[22] E. Sauvain, A. Shah, J. Hubin, Conference Record of the 21st IEEE Photovoltaics Specialists Conference, Orlando, (1990) 1560.

[23] C. Nicolet, D. Deribew, C. Renaud, G. Fleury, C. Brochon, E. Cloutet, L. Vignau, G. Wantz, H. Cramail, M. Geoghegan, G. Hadziioannou, J. Phys. Chemistry B, (2011) 12717.